Available online at www.sciencedirect.com
SCIENCE DIRECT®
Applied Catalysis A: General 248 (2003) 169–180
APPLIED CATALYSIS A: GENERAL
www.elsevier.com/locate/apcata

Preparation and characterization of In_2O_3-TiO_2 and V_2O_5/In_2O_3-TiO_2 composite oxides for catalytic applications

Benjaram M. Reddy*, Ibram Ganesh, Ataullah Khan

Inorganic and Physical Chemistry Division, Indian Institute of Chemical Technology, Uppal Road, Hyderabad 500007, India

Received 7 January 2003; received in revised form 17 February 2003; accepted 17 February 2003

Abstract

In_2O_3-TiO_2 (1:13 mole ratio) mixed oxide was prepared by a co-precipitation method with in situ generated ammonium hydroxide and was impregnated with various amounts of V_2O_5 (4–12 wt.%). The In_2O_3-TiO_2 and V_2O_5/In_2O_3-TiO_2 samples were subjected to thermal treatments from 773 to 1073 K and were investigated by X-ray diffraction, FT-infrared, and BET surface area methods to establish the effects of vanadia loading and thermal treatments on the surface structure of the dispersed vanadium oxide species and temperature stability of these catalysts. Characterization results suggest that the co-precipitated In_2O_3-TiO_2 is in X-ray amorphous state and exhibits reasonably high specific surface area. The In_2O_3-TiO_2 also accommodates a monolayer equivalent of V_2O_5 (12 wt.%) in a highly dispersed state. The V_2O_5/In_2O_3-TiO_2 catalyst is thermally stable up to 873 K calcination temperature. When subjected to thermal treatments beyond 873 K, the dispersed vanadium oxide selectively interacts with In_2O_3 portion of the mixed oxide and forms $InVO_4$ compound. The remaining TiO_2 appears in the form of anatase or rutile phase. These samples were evaluated for one step synthesis of 2,6-dimethylphenol from cyclohexanone and methanol mixtures in the vapour phase at normal atmospheric pressure. The 12% V_2O_5/In_2O_3-TiO_2 catalyst exhibits good conversion and product selectivity among various samples investigated.

Keywords: Titanium oxide; Indium oxide; Mixed oxide; In_2O_3-TiO_2; V_2O_5; Dispersion; Acid–base properties; Redox properties; Cyclohexanone; Methanol; 2,6-Dimethylphenol

1. Introduction

Titania has been widely employed as a support as well as catalyst for variety of applications [1]. The vanadium-titanium oxides are the basic components of industrial catalysts for selective catalytic reduction (SCR) of nitrogen oxides, selective oxidation of various hydrocarbons, and ammoxidation of N-heteroaromatic compounds [2–5]. In particular, titania anatase has been extensively used for several photocatalytic reactions for elimination of many organic pollutants from waste-waters [6,7]. Titania-based catalysts were also employed for HCN and COS hydrolysis, olefin epoxidations [8], and precious metal (Pt, Rh or Ru) or Ni-impregnated titania for Fischer–Tropsch synthesis [9]. The TiO_2 has also been used as an oxygen sensor to monitor automobile engine performance [10]. Numerous other reactions such as oxidation of H_2S to SO_2, dehydration of alcohols, isomerisation, and alkylation have also been studied by employing TiO_2 catalysts [1,10,11]. However, there are some disadvantages associated with TiO_2 which include low specific surface area, poor thermal stability, poor

* Corresponding author. Tel.: +91-40-2717-5406; fax: +91-40-2716-0921.
E-mail addresses: bmreddy@iict.ap.nic.in, mreddyb@yahoo.com (B.M. Reddy).

0926-860X/$ – see front matter © 2003 Elsevier Science B.V. All rights reserved.
doi:10.1016/S0926-860X(03)00157-1

mechanical strength, and lack of abrasion resistance. Therefore, several efforts can be found in the literature to increase the specific surface area and thermal stability of TiO_2 anatase structure by introducing various metals or non-metals into the titania matrix [1,12–22].

The In_2O_3-doped Al_2O_3 has been reported to show good activity for NO_x reduction as well as high resistance to H_2O and SO_2 poisoning in lean conditions [23,24]. Kikuchi et al. [25] introduced indium into various zeolites and reported a high activity and selectivity for NO_x reduction. Hamada et al. [26] used indium oxide-doped sol–gel alumina catalysts for various other applications. Recently, indium oxide promoted titanium oxides have been applied for different purposes such as photoelectrodes, transparent and conductive thin films in electronic and optoelectronic applications, and hydrogen production by photoassisted electrolysis of H_2O [27,28]. In view of their significance, a comprehensive investigation was undertaken by the authors to fully understand the evolution and physicochemical characteristics of In_2O_3-TiO_2 complex oxide systems. The primary objective of the present investigation was to provide basic insights into the structure of In_2O_3-TiO_2 and V_2O_5/In_2O_3-TiO_2 catalysts, shedding light on the influence of thermal treatments, oxide loading, and preparation method on both thermal stability and physicochemical characteristics of these materials. In this study, an indium-titanium mixed oxide was prepared by a homogeneous co-precipitation method with in situ generated ammonium hydroxide and was impregnated with various amounts of vanadium pentoxide. The In_2O_3-TiO_2 and V_2O_5/In_2O_3-TiO_2 samples were subjected to thermal treatments from 773 to 1073 K and were investigated by TGA–DTA, XRD, FTIR, and BET surface area methods. The catalytic properties of these composite oxides were evaluated for one step synthesis of 2,6-dimethylphenol from methanol and cyclohexanone mixtures in vapor phase.

2. Experimental section

2.1. Catalyst preparation

The In_2O_3-doped TiO_2 (1:13 molar ratio based on oxides) was prepared by a homogeneous co-precipitation method with in situ generated ammonium hydroxide [16]. In a typical experiment, the required quantities of indium chloride (Aldrich, AR grade) and titanium tetrachloride (Fluka, AR grade), dissolved separately in deionized water, were mixed together (pH 2). An excess amount of solid urea with a metal to urea molar ratio of 1:2.5 was also added to this mixture solution. To make $TiCl_4$ solution, the cold concentrated $TiCl_4$ was first digested in cold concentrated HCl and then diluted with doubly distilled water. The indium chloride was dissolved in ethanol before mixing with titanium chloride solution. The mixture solution was heated slowly to 363–368 K on a hot plate with vigorous stirring. In about 6 h of heating, as decomposition of urea progressed to certain extent, the formation of precipitate gradually occurred and pH of the solution increased to 7–8. In order to make total precipitation of the constituent metals sure, the pH of the solution was increased to 8.5 by adding dilute ammonia solution. The precipitate was heated for 6 h more to facilitate aging. The resulting precipitate was filtered off, washed several times with deionized water until no chlorides could be detected in the filtrate. The resulting cake was oven dried at 393 K for 16 h and finally calcined at 773 K for 6 h in a closed electrical furnace. Some portions of the calcined In_2O_3-TiO_2 were once again heated at 873, 973, and 1073 K for 6 h in a closed electrical furnace in air atmosphere.

The V_2O_5/In_2O_3-TiO_2 catalyst, containing various amounts of V_2O_5 (4–12 wt.%) was prepared by a standard wet impregnation method. The requisite quantity of ammonium metavanadate (Fluka, AR grade) was dissolved in aqueous oxalic acid (2 M) solution. To this clear solution, finely powdered calcined (773 K) support was added. The excess water was evaporated on a water bath and the resulting material was oven dried at 383 K for 12 h and subsequently calcined at 773 K for 6 h under the flow of dry oxygen. Some portions of the finished catalyst were once again heated at 873, 973, and 1073 K for 6 h in a closed electrical furnace in air atmosphere.

2.2. Catalyst characterization

The X-ray powder diffraction patterns have been recorded on a Siemens D-5000 diffractometer by using Cu Kα radiation source and Scintillation Counter detector. The XRD phases present in the samples were identified with the help of ASTM Powder Data Files.

The crystallite size of TiO_2 anatase and rutile were estimated with the help of Debye–Scherrer equation using the XRD data of anatase (0 1 0) and rutile (1 1 0) reflections [29]. The FTIR spectra were recorded on a Nicolet 740 FTIR spectrometer at ambient conditions, using KBr disks, with a normal resolution of $4\,cm^{-1}$ and averaging 100 spectra. A conventional all glass volumetric high vacuum (up to 1×10^{-6} Torr) system was used for BET surface area measurements. The BET surface area was measured by nitrogen physisorption at liquid nitrogen temperature (77 K) by taking $0.162\,nm^2$ as the area of cross-section of N_2 molecule.

2.3. Catalyst evaluation

The one step synthesis of 2,6-dimethylphenol was investigated in vapor phase under normal atmospheric pressure, in a down flow fixed bed differential microreactor, at different temperatures. In a typical experiment, ca. 0.5–2.0 g of a catalyst sample was secured between two plugs of Pyrex glass wool inside the glass reactor (Pyrex glass tube i.d. 0.8 cm) and above the catalyst bed filled with glass chips in order to act as preheating zone. The reactor was placed vertically inside a tubular furnace, which can be heated electrically. The reactor temperature was monitored by a thermocouple with its tip located near the catalyst bed and connected to a temperature indicator–controller. The catalyst was heated in a flow of air at 723 K for 5 h, prior to the reaction. The mixture of methanol and cyclohexanone was fed from a motorised syringe pump (Perfusor Secura FT, Germany) into the vaporizer where it was allowed to mix uniformly with air or nitrogen before entering the preheating zone of the reactor. The liquid products collected through spiral condensers in ice-cooled freezing traps, were analysed by a gas chromatograph. The liquid products were quantified by FID with a 10% Carbowax 20 M (length 2 m) column. The main products observed were 2,6-dimethylphenol, 2,6-dimethylcyclohexanone, 2-methylcyclohexanone, 1-methoxycyclohexene and some unidentified products. At higher temperatures some small amounts of CO and CO_2 were also noticed. The activity data were collected under steady-state conditions. The conversion, selectivity, and yield were calculated as per the procedure described elsewhere [30].

3. Results and discussion

The co-precipitated In_2O_3-TiO_2 sample was subjected to DTA–TGA analysis before calcination. The obtained thermogram as presented in Fig. 1 reveals a major and a minor weight loss peak. The major low temperature peak in the range 309–393 K is primarily due to loss of non-dissociate adsorbed water as well as water held on the surface by hydrogen bonding. Rapid

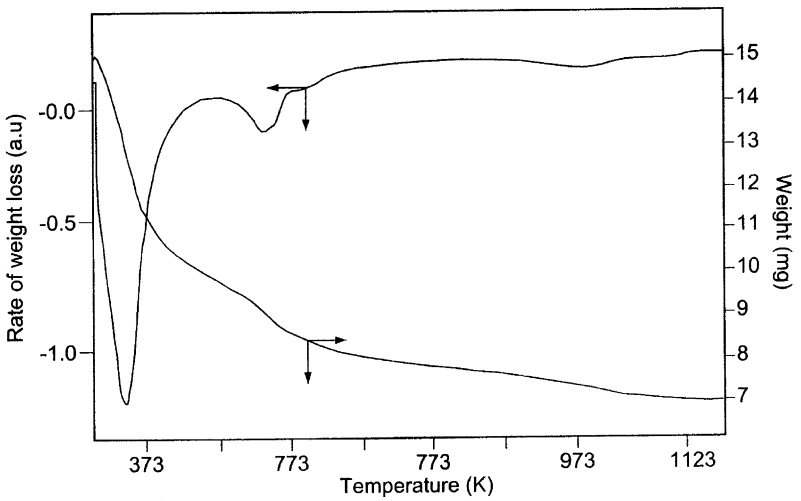

Fig. 1. TGA and DTA profile of In_2O_3-TiO_2 sample before calcination.

loss of water occurs around 498–548 K due to dehydroxylation of the surface. The percentage weight loss between ambient and 773 K is about 48.2%, which suggests that dehydration of hydroxyl groups could be responsible for this weight loss. However, in the temperature range between 773 and 1173 K the weight loss is only about 5.6%. It suggests that over this temperature range the In_2O_3-doped TiO_2 support is quite thermally stable.

The BET surface area of In_2O_3-TiO_2 and V_2O_5/In_2O_3-TiO_2 samples calcined at different temperatures is depicted in Fig. 2. The necessary quantity of vanadia to cover the support surface as a two-dimensional monomolecular layer can be estimated from structural calculations [15]. From V–O bond lengths of crystalline V_2O_5, the monolayer surface coverage is estimated to be 0.145 wt.% $V_2O_5\,m^{-2}$ of the support. However, the monolayer coverage depends not only on the support surface area but also on the concentration of reactive surface hydroxyl groups apart from other preparative variables [4,12,31]. Therefore, a range of V_2O_5 contents from 4 to 12 wt.% were selected in the present investigation. As can be seen from Fig. 2, there is a considerable decrease in the specific surface area of the samples with increasing calcination temperature, which can be due to sintering of the samples at higher calcination temperatures. Another interesting point to be noted from Fig. 2 is that the decrease

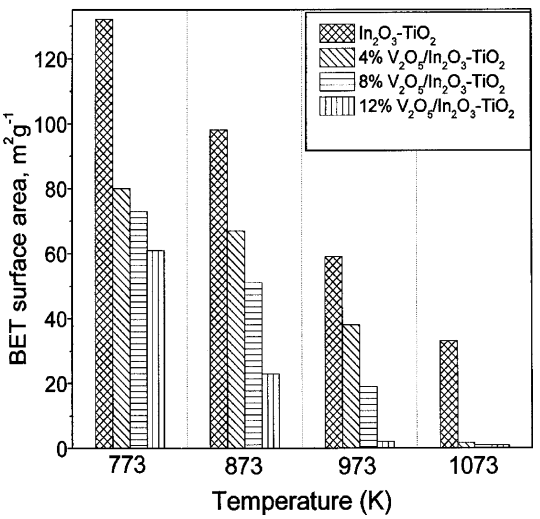

Fig. 2. Effect of calcination temperature on the BET surface area of In_2O_3-TiO_2 and V_2O_5/In_2O_3-TiO_2 samples.

is more in the case of vanadia-impregnated samples than pure support. The decrease in the specific surface area with increase in V_2O_5 loading at a given temperature is primarily due to narrowing of the pore diameter of the support by the dispersed vanadium oxide as well as solid-state reactions between the active component and the supporting oxides [4,20,21]. The XRD results presented in the subsequent paragraphs support the later possibility.

X-ray powder diffraction patterns of In_2O_3-TiO_2 sample calcined at various temperatures are shown in Fig. 3. As can be noted from this figure, the In_2O_3-TiO_2 support calcined at 773 K is in a poorly crystalline state exhibiting broad diffraction lines due to TiO_2 anatase phase (JCPDS Files No. 21-1272). With increase in calcination temperature from 773 to 973 K, in addition to an increase in the intensity of the lines due to anatase phase, presence of new broad peaks at $d = 2.92$, 1.79, and 2.53 Å can be seen, which can be attributed to In_2O_3 (JCPDS Files No. 6-416). On further increase of calcination temperature from 973 to 1073 K an increase in the intensity of the lines due to both anatase and In_2O_3 can be seen. Very interestingly, no diffraction lines due to TiO_2 rutile phase (JCPDS Files No. 21-1276) or compounds between TiO_2 and In_2O_3 are observed. Thus, In_2O_3-doped TiO_2 appears to contain mainly the anatase phase along with In_2O_3 and is quite stable up to the calcination temperature of 1073 K.

The XRD profiles of 4 and 12% V_2O_5/In_2O_3-TiO_2 catalysts calcined at different temperatures from 773 to 1073 K are shown in Figs. 4 and 5, respectively. Similar results were also noted in the case of 8% V_2O_5/In_2O_3-TiO_2 catalysts. As can be observed from Fig. 4, there are no lines either due to V_2O_5 or to a compound between the vanadia and In_2O_3 or TiO_2 up to a calcination temperature of 873 K, except some broad diffraction lines due to anatase as well as In_2O_3. The XRD results thus indicate that vanadium oxide is in a highly dispersed or amorphous state on the surface of the support up to 873 K calcination temperature. On further increase of calcination temperature from 873 to 973 K, in addition to sharp lines due to both anatase and In_2O_3, some new peaks with less intensity can be seen at $d = 2.70$, 2.53, and 1.51 Å. These lines could be attributed to the formation of γ-$InVO_4$ (JCPDS Files No. 31-605). On further increase of calcination temperature from 973 to 1073 K, a further

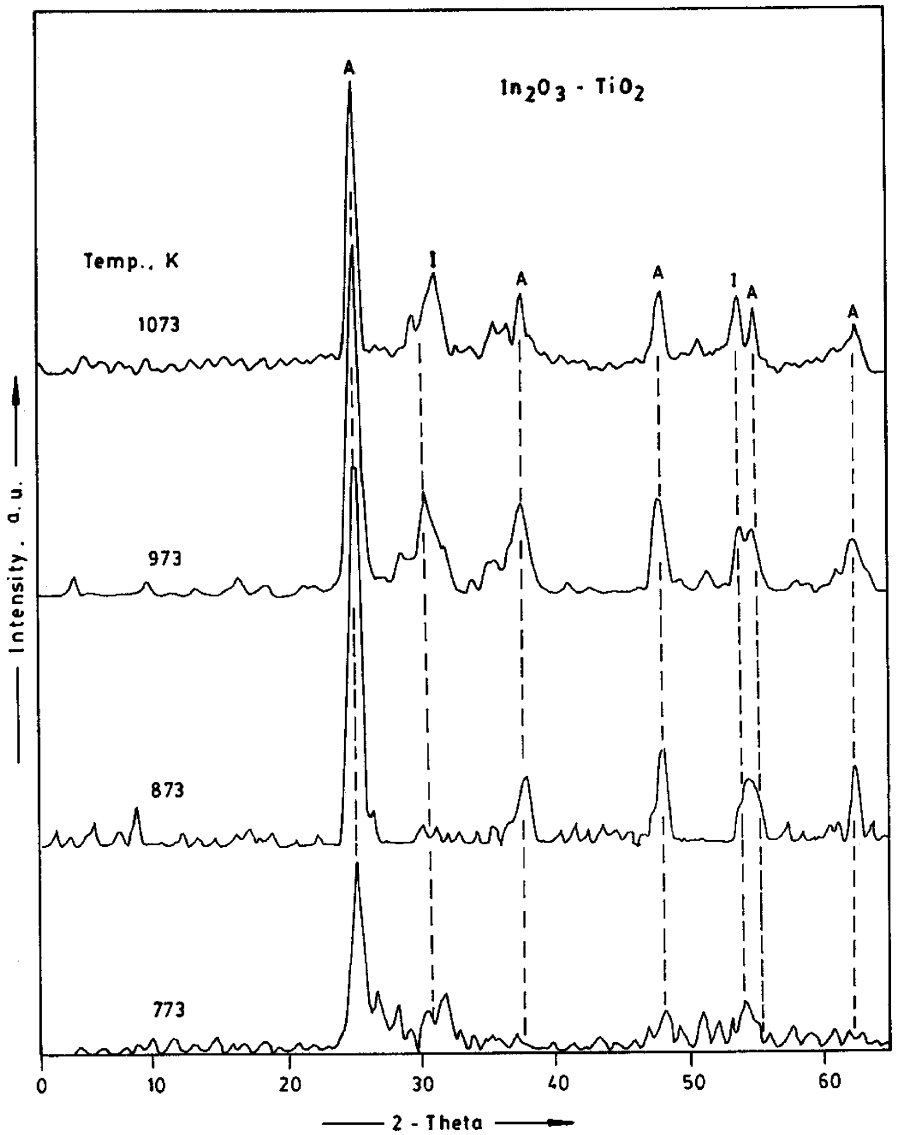

Fig. 3. X-ray powder diffraction patterns of In_2O_3-TiO_2 calcined at different temperatures: (A) lines due to anatase; (I) lines due to In_2O_3.

improvement in the intensity of the lines due to anatase, In_2O_3, and γ-$InVO_4$ can be observed. Interestingly, few new lines pertaining to TiO_2 rutile phase can be seen at 1073 K due to partial phase transformation of TiO_2 anatase into rutile (∼10%). It is an established fact in the literature that for V_2O_5 contents of less than monolayer coverage the dispersed vanadium oxide will be present as a two-dimensional overlayer on the support [4,5,31]. Quantities in excess of monolayer coverage will have microcrystalline V_2O_5 particles in addition to the surface vanadium oxide overlayer. An interesting observation to be noted from Fig. 4 is that crystallisation of γ-$InVO_4$ compound at 973 K, which is expected to be formed at the expense of the dispersed vanadium oxide on the In_2O_3-TiO_2 surface.

In the case of 8% V_2O_5/In_2O_3-TiO_2 catalyst (not shown), the presence of weak lines due to γ-$InVO_4$

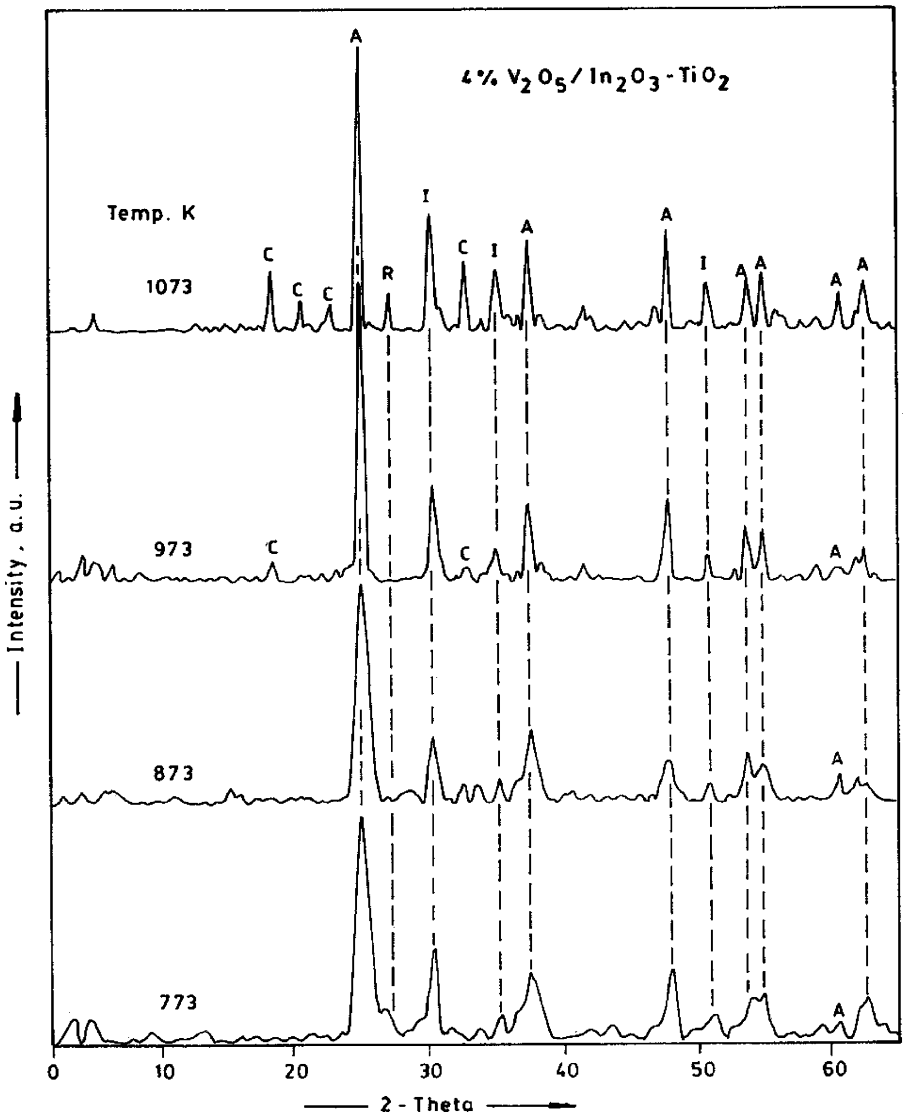

Fig. 4. X-ray powder diffraction patterns of 4 wt.% V_2O_5/In_2O_3-TiO_2 calcined at different temperatures: (A) lines due to anatase; (R) lines due to rutile; (I) lines due to In_2O_3; (C) lines due to $InVO_4$.

were observed at the calcination temperature of 873 K, along with intense lines due to anatase and In_2O_3. A significant improvement in the intensity of the lines due to anatase and γ-$InVO_4$ phases were noted with increasing calcination temperature from 873 to 1073 K. In the case of 12% V_2O_5/In_2O_3-TiO_2 catalyst (Fig. 5), the presence of intense lines due to γ-$InVO_4$ can be seen even at the calcination temperature of 873 K, in addition to the lines of anatase and In_2O_3. On further increase of calcination temperature from 873 to 1073 K, an appreciable improvement in the intensity of lines due to γ-$InVO_4$ along with anatase can be noted.

To understand the influence of indium oxide on the phase transformation and crystallite growth of anatase, the crystallite size in various samples was estimated using X-ray line broadening method and presented in Table 1. The In_2O_3-TiO_2 mixed oxide support contains

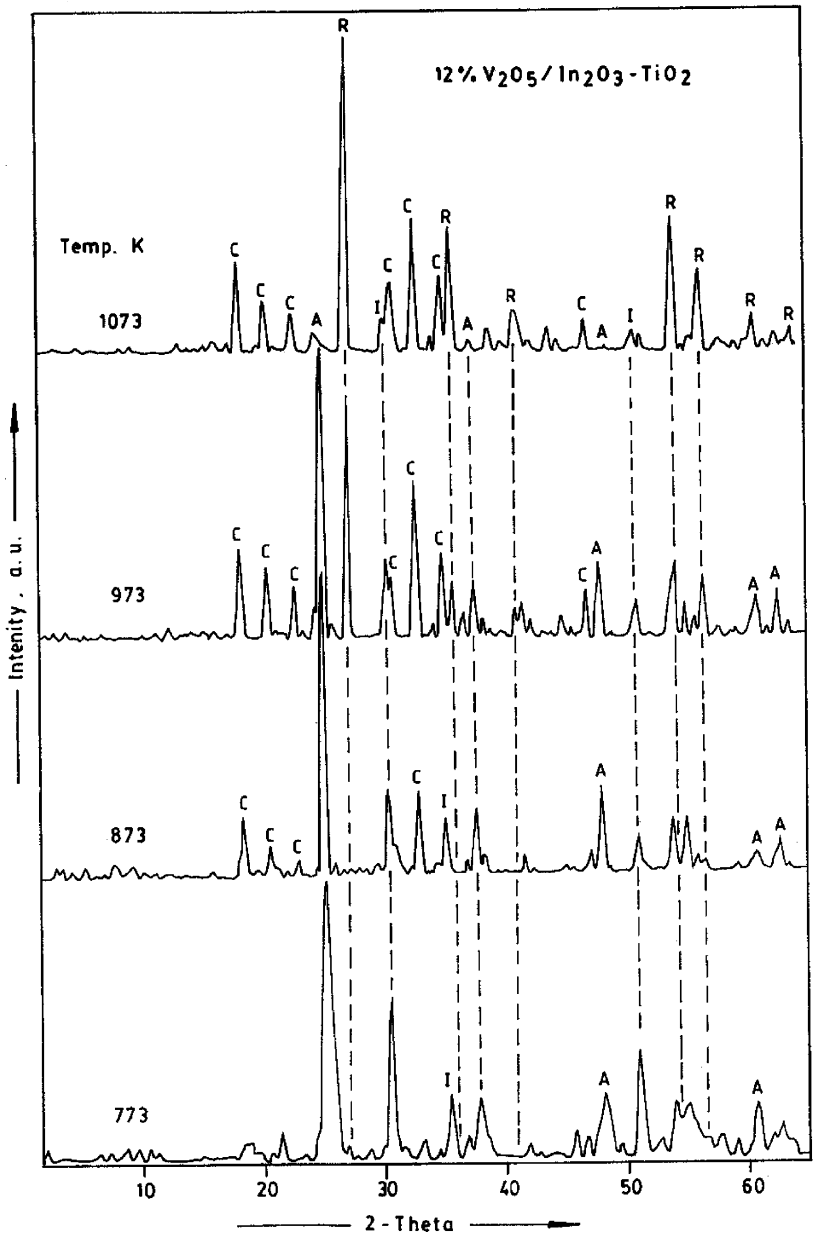

Fig. 5. X-ray powder diffraction patterns of 12 wt.% V_2O_5/In_2O_3-TiO_2 calcined at different temperatures: (A) lines due to anatase; (R) lines due to rutile; (I) lines due to In_2O_3; (C) lines due to $InVO_4$.

only anatase phase and whose crystallite size increases with increasing calcination temperature. In the case of V_2O_5-containing catalysts, both anatase and rutile phases are present. As the vanadia loading increases, the crystallite size of both anatase and rutile phases increase progressively. From Table 1, it is clear that addition of indium oxide retards the anatase to rutile phase transformation which is normally expected to occur at 823 K and above calcination temperatures in impurity-free TiO_2 samples [4,16]. It can be noted

Table 1
Crystallite size (nm) measurements of TiO_2 anatase (A) and rutile (R) phases in In_2O_3-TiO_2 and V_2O_5/In_2O_3-TiO_2 samples calcined at different temperatures

Temperature (K)	In_2O_3-TiO_2		4% V_2O_5/In_2O_3-TiO_2		8%V_2O_5/In_2O_3-TiO_2		12%V_2O_5/In_2O_3-TiO_2	
	A	R	A	R	A	R	A	R
773	9.3	–	9.7	–	9.2	–	11.5	–
873	10.4	–	11.4	–	12.7	–	25.6	–
973	11.0	–	21.6	–	20.0	–	28.3	25.4
1073	26.7	–	26.4	28.1	–	38.4	–	28.2

from Table 1 that impregnated vanadia accelerates the grain growth of anatase and its subsequent phase transformation into rutile.

A closer examination of Figs. 3–5 reveals that thermal treatments and impregnation of V_2O_5 have major influence on the properties of In_2O_3-TiO_2 support:

(1) The In_2O_3-TiO_2 mixed oxide support prepared by a homogeneous co-precipitation method is quite stable in terms of phases and chemical composition up to 1073 K calcination temperature in the absence of V_2O_5. This is evidenced by the absence of TiO_2 rutile, which can be expected at 823 K and above temperatures in impurity-free TiO_2 samples [16]. Hence, it can be inferred that presence of indium oxide retards the phase transformation of anatase to rutile in In_2O_3-TiO_2 samples.
(2) Absence of crystalline V_2O_5 phase and appearance of $InVO_4$ compound accompanied by TiO_2 anatase or rutile phases for calcination temperatures beyond 773 K. Further, the intensity of the lines due to both $InVO_4$ and TiO_2 (anatase and/or rutile) phases also increase with increasing calcination temperature.
(3) Very interestingly, the anatase phase of titania is stable up to 973 K even in the presence of vanadia (Fig. 4).

The XRD observations described above reveal an interesting information about the reactivity of vanadia towards In_2O_3-TiO_2 mixed oxide. It appears from XRD results that vanadia reacts preferentially with In_2O_3 portion of the In_2O_3-TiO_2 to form $InVO_4$ thus liberating TiO_2. The portion of TiO_2 released from In_2O_3-TiO_2 composite oxide appears as crystalline anatase or rutile phases as shown in the following equation:

$$In_2O_3\text{-}TiO_2 + V_2O_5 \rightarrow 2\gamma\text{-}InVO_4 + TiO_2 \text{ (anatase and rutile)} \quad (1)$$

It is an established fact in the literature [4,14,15,32] that highly dispersed vanadia on TiO_2 support accelerates the anatase-to-rutile phase transformation by lowering the activation temperature of this phenomenon [16]. During this phase transformation some of the dispersed vanadia is normally reduced and gets incorporated into the rutile structure as $V_xTi_{(1-x)}O_2$ (rutile solid solution) [4,14,15,32]. However, in the case of In_2O_3-TiO_2 mixed oxide, the reactivity of vanadia towards In_2O_3-TiO_2 appears to be quite different. It interacts preferably with the In_2O_3 portion of the support to form γ-$InVO_4$ as shown in Eq. (1). A similar preferential interaction of vanadia with Ga_2O_3 or La_2O_3 portions of the Ga_2O_3-TiO_2 and La_2O_3-TiO_2 mixed oxides was also noted earlier [21,22].

The FTIR spectra of In_2O_3-TiO_2 mixed oxide support calcined from 773 to 1073 K revealed the presence of strong absorption bands between 3400 and 3600 cm^{-1} and at 1625 cm^{-1}. In addition, a new peak at 650–830 cm^{-1} was also observed in the case of 1073 K calcined sample. The absorption peaks between 3400 and 3600 cm^{-1}, known to be due to the presence of surface hydroxyl groups, were gradually decreased with increasing calcination temperature [33]. The peak at 1625 cm^{-1}, due to the deformation vibrations of adsorbed water, was also gradually decreased after calcination at high temperatures [34]. Anatase and rutile phases of titania exhibit strong absorption bands in the region of 850–650 and 800–650 cm^{-1}, respectively [35]. A gradual improvement in the region between 850 and 650 cm^{-1} with increasing calcination temperature was noted

suggesting that the titania is gradually transforming from an amorphous to a crystalline anatase phase in line with XRD observations.

The FTIR spectra of various V_2O_5/In_2O_3-TiO_2 catalysts calcined at different temperatures were recorded in the range 400–1800 cm^{-1}, where those bands due to $\nu_{V=O}$ are expected to be observed. Normally, the IR spectrum of pure crystalline V_2O_5 shows sharp absorption bands at 1020 and another at 820 cm^{-1} due to V=O stretching and V–O–V deformation modes, respectively [4]. The spectrum of 4 wt.% V_2O_5/In_2O_3-TiO_2 sample calcined at 773 K was identical to that of pure support, in agreement with the XRD observations, where only the anatase phase of TiO_2 was noted. With increase in calcination temperature from 773 to 1073 K, a gradual change from amorphous to a crystalline anatase formation was noted from FTIR in line with XRD results. A weaker band at around 980 cm^{-1} was noted in the spectrum of the sample calcined at 873 K. On further increase of calcination temperature from 873 to 1073 K, the absorption band in the region 990–960 cm^{-1} completely diminished suggesting that the dispersed vanadium oxide is transformed from amorphous VO_x to a different form. However, no absorption bands at 1020 and 820 cm^{-1} due to V=O stretching and deformation modes of crystalline V_2O_5 were seen. The band in the range 990–960 cm^{-1} has been reported for vanadia-titania catalysts having vanadium content close to monolayer coverage [4]. Nakagawa et al. [36] reported that the V=O stretching frequency is sensitive to vanadium oxide loading and found a shift from 1020 (pure V_2O_5) to 980 cm^{-1} thus indicating that vanadium oxide is present as an amorphous VO_x at low coverages, and both amorphous and crystalline V_2O_5 at high surface coverages. The disappearance of absorption band at 990–960 cm^{-1} was also noted in the case of 8 and 12% V_2O_5/In_2O_3-TiO_2 samples at 873 K and above calcination temperatures. The formation of crystalline $InVO_4$ may be the reason for the disappearance of the absorption band at 990–960 cm^{-1} of the dispersed VO_x species [36]. Thus, all the observations made from FTIR were in agreement with the findings of XRD study.

2,6-Dimethylphenol is an important chemical intermediate in the polymer industry for engineering plastics [37]. The commercial synthetic method was based on a liquid phase process, where phenol is methylated with methanol using an alumina catalyst. However, this process not only requires high pressure and temperature, but also produces wide range of byproducts, including various isomers of xylenol [38]. Therefore, there are several advantages like continuous production, simplified product recovery, catalyst regenerability, etc. for carrying out this reaction in the vapour phase from cyclohexanone and methanol. Wang et al. [39] reported the synthesis of 2,6-dimethylphenol from methanol and cyclohexanone over vanadia-titania catalysts. However, the conversion and product selectivities reported are limited on this catalyst. Recently, mixed oxide supports have attracted much attention because of their better performance than their constituent single oxides for various reactions [20,40,41]. Therefore, this particular reaction was selected in the present investigation to study the catalytic properties of In_2O_3-TiO_2 and V_2O_5/In_2O_3-TiO_2 oxides.

The activity and selectivity of various samples was investigated between 573 and 698 K. The activity and selectivity trends on various catalysts followed the same pattern with temperature. In general, an increase in the conversion with an increase in temperature was observed. Formation of some additional side products with traces of CO and CO_2 were also occasionally noted at higher reaction temperatures. The change in conversion as a function of contact time at a fixed temperature of 673 K was also studied on various catalysts. A decrease in the conversion of cyclohexanone during the initial reaction period was noted for all the catalysts used, but stable activity was obtained within few hours. The conversion and selectivity were calculated on cyclohexanone basis and almost all the excess methanol was recovered after the reaction. The conversion and selectivity results as a function of temperature over In_2O_3-TiO_2 and 12% V_2O_5/In_2O_3-TiO_2 samples calcined at 773 K are presented in Figs. 6 and 7, respectively. Similar trends were also noted on 4 and 8% catalysts. However, these samples exhibited less product yield than the 12% V_2O_5/In_2O_3-TiO_2 sample.

As can be noted in Fig. 6, the conversion of cyclohexanone increases with increasing reaction temperature over the In_2O_3-TiO_2 sample. At low reaction temperatures the formation of 1-methoxycyclohexene in large amounts is noted in addition to small amounts of

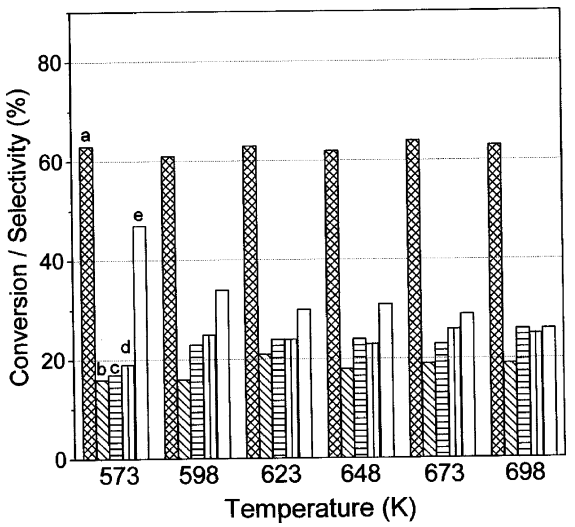

Fig. 6. Activity and selectivity results of one step synthesis of 2,6-dimethylphenol from cyclohexanone and methanol over In_2O_3-TiO_2 at different temperatures: (a) conversion; (b) selectivity to 2,6-dimethylphenol; (c) 2,6-dimethylcyclohexanone; (d) 2-methylcyclohexanone; (e) 1-methoxycyclohexene.

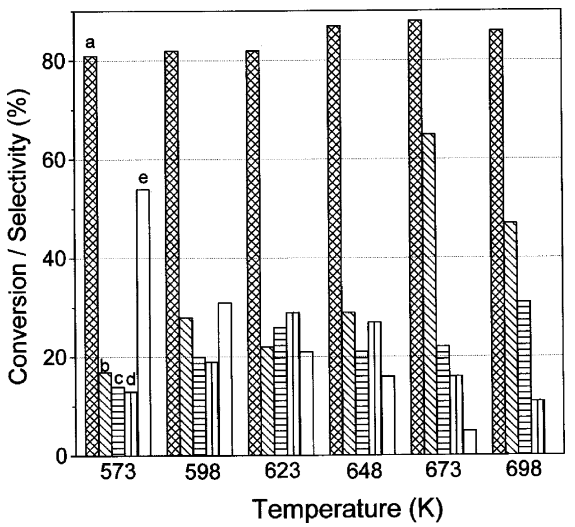

Fig. 7. Activity and selectivity results of one step synthesis of 2,6-dimethylphenol from cyclohexanone and methanol over 12 wt.% V_2O_5/In_2O_3-TiO_2 at different temperatures: (a) conversion; (b) selectivity to 2,6-dimethylphenol; (c) 2,6-dimethylcyclohexanone; (d) 2-methylcyclohexanone; (e) 1-methoxycyclohexene.

2-methylcyclohexanone, 2,6-dimethylcyclohexanone, and 2,6-dimethylphenol. The selectivity towards 2-methylcyclohexanone, 2,6-dimethylcyclohexanone and 2,6-dimethylphenol increased with increasing reaction temperature and at the same time selectivity towards 1-methoxycyclohexene decreased drastically. As reaction temperature increases the selectivity towards 2,6-dimethylphenol increased slightly. However, at all temperatures the formation of methyl formate, dimethylether, and CO_x in small quantities was noted. Upon impregnating the support with V_2O_5 a major change in the product distribution was noticed. Over vanadia-containing catalysts the maximum selectivity of 2,6-dimethylphenol was noted at 673 K (Fig. 7). In general, the selectivity of 2,6-dimethylphenol was found to increase with increasing reaction temperature at the same time the selectivity towards 2,6-dimethylcyclohexanone, 2-methylcyclohexanone, and 1-methoxycyclohexene decreased. The selectivity towards 2,6-dimethylphenol was high in all vanadia-impregnated samples when compared to that of pure support. The activity results suggest that 12% V_2O_5/In_2O_3-TiO_2 catalyst exhibits more 2,6-dimethylphenol yield (58%) and seem to be a promising catalyst for this reaction [42–46]. To the best of our knowledge, there are only a few reports in the open literature on the synthesis of 2,6-dimethylphenol from cyclohexanone and methanol in vapour phase. In particular, Wang and coworkers [43–45] investigated the synthesis of 2,6-dimethylphenol from methanol and cyclohexanol or a mixture of cyclohexanol and cyclohexanone (KA-oil) over a Cr/MgO catalyst and reported about 54% yield at 673 K. A slight improvement in the activity of Cr/MgO catalyst was also noted up on addition of Pt promoter to Cr/MgO catalyst [46]. The better activity of 12% V_2O_5/In_2O_3-TiO_2 catalyst in the present study could be due to various factors such as a high specific surface area of the sample, a reasonably large quantity of V_2O_5 in a highly dispersed state, and combined acid–base and redox properties together in this complex catalyst system. However, further studies are required to understand the nature and surface structure of these catalysts and their potential use. Of course, the formation of 2,6-dimethylphenol from methanol and cyclohexanone is a complex reaction and proceeds in a different manner from that of normal methylation of aromatic compounds [20,47].

As envisaged earlier, in the first step of reaction the cyclohexanone condenses with a methanol molecule, in its another isomeric form enol, and produces 1-methoxycyclohexene, which is observed as one of the side products [20]. Thus, 1-methoxycyclohexene formed over isomerisation produces 2-methylcyclohexanone. Thus, 2-methylcyclohexanone formed by condensing with another molecule of methanol produces 2,6-dimethylcyclohexanone. The formed 2,6-dimethylcyclohexanone by oxidative dehydrogenation probably produces the 2,6-dimethylphenol. However, detailed studies are highly essential to establish the mechanism of this complex reaction. It is an established fact in the literature that transition metal oxides, such as V_2O_5, MoO_3, etc. are very active for the oxidative dehydrogenation of organic molecules [31,48]. The mixed oxide supports when doped with a redox metal oxide are expected to show better catalytic properties [20,31,49]. Recently, Deo and Wachs [50] investigated methanol oxidation on a number of supported vanadium oxide catalysts. They found that the activity of the alcohol oxidation correlates with the extent of reduction and strength of V=O and V–O–M bonds. However, it is difficult to establish such a direct correlation in the present study because of the complexity of the reaction mechanism.

4. Conclusions

The following conclusions can be drawn from the present study:

(1) The In_2O_3-TiO_2 binary oxide is an interesting support for the dispersion of vanadium oxide.
(2) The co-precipitated In_2O_3-TiO_2 mixed oxide when calcined at 773 K is in X-ray amorphous state and exhibits reasonably high specific surface area.
(3) The In_2O_3-TiO_2 mixed oxide also accommodates a monolayer equivalent (12 wt.%) of V_2O_5 in a highly dispersed state on its surface. Further, the V_2O_5/In_2O_3-TiO_2 catalyst is also thermally stable up to 873 K calcination temperature. The V_2O_5 selectively interacts with In_2O_3 portion of the In_2O_3-TiO_2 mixed oxide and readily forms γ-$InVO_4$ compound with the liberation of TiO_2 when subjected to thermal treatments beyond 873 K. The liberated TiO_2 appears in the form of anatase as well as rutile phases.
(4) Interestingly, the 12% V_2O_5/In_2O_3-TiO_2 mixed oxide catalyst exhibits better catalytic properties for the vapour phase synthesis of 2,6-dimethylphenol from methanol and cyclohexanone mixtures. A high activity of this catalyst could be related to more quantity of V_2O_5 in a highly dispersed state apart from acid–base and redox properties of the catalyst.

Further studies are essential to understand the mechanism of this reaction and commercial viability of these catalysts.

Acknowledgements

Ataullah Khan thanks Department of Science and Technology, New Delhi for a Junior Research Fellowship under SERC Scheme (SP/S1/H-20/98).

References

[1] K.I. Hadjiivanov, D.G. Klissurski, Chem. Soc. Rev. 25 (1996) 61, and references therein.
[2] J.C. Vedrine (Ed.), Eurocat oxide, Catal. Today 20 (1994) 1, and references therein.
[3] H. Bosh, F. Janssen, Catal. Today 2 (1988) 369.
[4] G.C. Bond, S.F. Tahir, Appl. Catal. 71 (1991) 1, and references therein.
[5] G. Deo, I.E. Wachs, J. Haber, Crit. Rev. Surf. Chem. 4 (1994) 141, and references therein.
[6] M.R. Hoffmann, S.T. Martin, W. Choi, D.W. Bahnenann, Chem. Rev. 69 (1995) 95.
[7] M. Apno, Res. Chem. Intermed. 11 (1989) 67.
[8] M. Taramasso, G. Perego, B. Notari, US Patent 4,410,501 (1983).
[9] M.A. Vannice, R.L. Garten, J. Catal. 56 (1979) 236.
[10] J. Whitehead, Titanium compounds, inorganic, in: M. Grayson (Executive Ed.), Kirk–Othmer Encyclopaedia of Chemical Technology, third ed., vol. 23, Wiley, New York, 1983, p. 131.
[11] K. Arata, K. Tanabe, Chem. Lett. (1979) 1017.
[12] A. Baiker, P. Dollenmeier, M. Glinski, A. Reller, Appl. Catal. 35 (1987) 351.
[13] H.M. Matralis, M. Ciardelli, M. Ruwet, P. Grange, J. Catal. 157 (1995) 368.
[14] R. Kozlowski, R.F. Pettifer, J.M. Thomas, J. Phys. Chem. 87 (1983) 5176.
[15] F. Roozeboom, M.C. Mittlemeijer-Hazeleger, J.A. Moulin, J. Medema, V.H.J. de Beer, P.J. Gellings, J. Phys. Chem. 84 (1980) 2783.

[16] S.R. Yoganarasimhan, C.N.R. Rao, Trans. Faraday Soc. 58 (1962) 1579.
[17] K.-N.P. Kumar, Appl. Catal. A: Gen. 119 (1994) 163.
[18] B.M. Reddy, B. Manohar, S. Mehdi, J. Solid State Chem. 97 (1992) 317.
[19] B.M. Reddy, I. Ganesh, E.P. Reddy, J. Phys. Chem. B 101 (1997) 1769.
[20] B.M. Reddy, I. Ganesh, J. Mol. Catal. A: Chem. 169 (2001) 207.
[21] B.M. Reddy, I. Ganesh, E.P. Reddy, A. Fernández, P.G. Smirniotis, J. Phys. Chem. B 105 (2001) 6227.
[22] B.M. Reddy, P.M. Sreekanth, E.P. Reddy, Y. Yamada, Q. Xu, T. Kobayashi, J. Phys. Chem. B 106 (2002) 5695.
[23] T. Miyadera, K. Yoshida, Chem. Lett. (1993) 1483.
[24] P.W. Park, C.S. Ragle, C.L. Boyer, M.L. Balmer, M. Engelhard, D.Mc. Cready, J. Catal. 210 (2002) 97.
[25] M. Ogura, M. Hayashi, E. Kikuchi, Catal. Today 45 (1998) 139.
[26] T. Maunula, Y. Kintaichi, M. Inaba, M. Haneda, K. Sato, H. Hamada, Appl. Catal. B: Environ. 15 (1998) 291.
[27] A.-W. Xu, Y. Gao, H.-Q. Lin, J. Catal. 207 (2002) 151.
[28] S.K. Poznyak, D.V. Talapin, A.I. Kulav, J. Phys. Chem. B 105 (2001) 4816, and references therein.
[29] H.P. Klug, L.E. Alexander, X-ray Diffraction Procedures for Polycrystalline and Amorphous Materials, second ed., Wiley, New York, 1974.
[30] B.M. Reddy, M.V. Kumar, K.J. Ratanam, Appl. Catal. A: Gen. 181 (1999) 77.
[31] B.M. Reddy, I. Ganesh, B. Chowdhury, Catal. Today 49 (1999) 115.
[32] B.M. Reddy, B. Manohar, E.P. Reddy, Langmuir 9 (1993) 1781.
[33] H.H. Kung, Transition metal oxides, surface chemistry and catalysis, Stud. Surf. Sci. Catal. 45 (1988) 57.
[34] A. Jentys, G. Warecka, M. Derewinski, J.A. Lercher, J. Phys. Chem. 93 (1989) 4837.
[35] R.A. Nyquist, L.L. Putzig, M.A. Leugers, Hand Book of Infrared and Raman Spectra of Inorganic Compounds and Organic Salts, Academic Press, New York, 1997.
[36] Y. Nakagawa, J. Ono, H. Miyata, Y. Kubokawa, J. Chem. Soc., Faraday Trans. 79 (1983) 2929.
[37] J.M. Margolis, Engineering Thermoplastics: Properties and Applications, Marcel Dekker, New York, 1985.
[38] K. Weissermel, H.-J. Arpe, Industrielle Organische Chemie, Chemie, GmbH, Weium, Germany, 1976.
[39] F.L. Wang, L. Yu, W.S. Lee, W.F. Wang, J. Chem. Soc., Chem. Commun. (1994) 811.
[40] I. Wang, R.C. Chang, J. Catal. 107 (1987) 195.
[41] B.E. Hand, M. Maciejewski, A. Baiker, J. Catal. 134 (1992) 75.
[42] I. Ganesh, Ph.D. Thesis, Osmania University, India, 1999.
[43] F.L. Wang, T.F. Tsai, Appl. Catal. A: Gen. 201 (2000) 91.
[44] F.L. Wang, T.F. Tsai, Y.H. Tsai, Y.K. Cheng, Appl. Catal. A: Gen. 126 (1995) L229.
[45] F.L. Wang, T.F. Tsai, Catal. Today 44 (1998) 259.
[46] F.L. Wang, T.F. Tsai, J. Chin. Chem. Soc. 47 (2000) 163.
[47] G.S. Devi, G. Giridhar, B.M. Reddy, J. Mol. Catal. A: Chem. 181 (2002) 173.
[48] A. Lisovski, C. Ahroni, Catal. Rev. Sci. Eng. 36 (1994) 25.
[49] B.M. Reddy, I. Ganesh, B. Chowdhury, Chem. Lett. (1997) 1145.
[50] G. Deo, I.E. Wachs, J. Catal. 156 (1994) 323.